

Formation of Small Aromatic Molecules in a Sooting Ethylene Flame

Stephen J. Harris

Anita M. Weiner

and

Richard J. Blint

Physical Chemistry Department, General Motors Research Laboratories, Warren, MI 48090-9055

Abstract

Small aromatic species are undoubtedly important precursor molecules in the formation of polycyclic aromatic hydrocarbons and soot, two important pollutants in diesel, direct-injection stratified charge (DISC), and other heterogeneous-combustion engines. Unfortunately, the chemical route to their formation is poorly understood, in part because rate constants for reactions of aromatic species at flame temperatures are largely unknown. In this work we used a quartz sampling probe to measure the concentration profiles of the single-ring aromatics benzene, phenylacetylene, and styrene in a heavily sooting premixed ethylene flame. A detailed chemical kinetics model was then constructed for the purpose of explaining the flame chemistry. The model, which uses estimated rate constants for many of the reactions involving aromatic species, gives good predictions for benzene and styrene and fair predictions for phenylacetylene. A sensitivity analysis has isolated a particular chemical reaction which controls their rate of formation, and it shows that even large errors in the other aromatic rate constants have relatively little effect on the predictions. Our approach will be applied in the future to trying to understand the formation of larger aromatic species and soot.

Introduction

Over the years there has been a considerable effort towards improving our understanding of the detailed chemistry in hydrocarbon combustion¹⁻³. Much of the work has concentrated on lean and stoichiometric flame environments, but understanding the processes that take place in rich systems is of great importance since many practical flames are diffusion flames. Unfortunately, rich combustion is a very difficult area for flame modeling because of the involvement of large hydrocarbon molecules and soot, species whose chemistry and thermodynamics are poorly known. In contrast, lean and near-stoichiometric flames involve a smaller number of species, nearly all of which are eventually converted to CO_2 and H_2O .

However, as knowledge of the kinetics and thermodynamics of hydrocarbons has increased, a growing number of studies have considered rich flame environments. These include, for example, the experiments of Homann and Wagner⁴, Howard and co-workers⁵, Bockhorn⁶, and Taylor⁷. In addition, detailed models have recently been constructed specifically to deal with rich flames⁸⁻¹⁰. In most of these cases, however, studies have been limited to non-sooting or lightly sooting flames because the presence of soot can make measurements difficult and because models have tended to avoid systems where pyrolysis chemistry and soot formation played major roles.

In recent work¹¹ we measured mole fraction profiles of a number of stable and radical species in a heavily sooting ethylene flame, and, building on previous work^{2,9,12}, we developed a model which predicted the profiles of many of the measured species with good accuracy. It would be very valuable to develop a reliable ethylene combustion model because many fuels such as octane are converted largely to ethylene on their way to being oxidized¹. Thus, an ethylene oxidation mechanism is an important component for models of more realistic fuels.

Unfortunately, our model severely underestimated the benzene mole fraction, and no other aromatic species was modeled. Since the goal of this research program is to understand the chemistry of soot formation, and since aromatic species undoubtedly play an important role in that process, our inability to model the chemistry of even the simplest aromatics was an important stumbling block. In this paper we describe modifications to our model which allow the successful prediction of the profiles of benzene, styrene, and, to a lesser extent, phenylacetylene. It is our hope that if the chemistry of large aromatics is similar to that of smaller aromatics, then semi-quantitative predictions of soot formation kinetics in well-studied systems such as premixed flat flames¹³ may be attainable in the foreseeable future.

Experiment and Model

The experimental conditions employed in this work have been described previously¹¹. Briefly, a flat premixed $\text{C}_2\text{H}_4/\text{O}_2/\text{Ar}$ flame with C/O ratio of 0.92 ($\phi = 2.76$) was stabilized on a water-cooled porous plug burner surrounded by a shroud of nitrogen. The $\text{Ar} : \text{O}_2$ mole ratio was 79 : 21. A quartz microprobe withdrew gases from the flame. No measurements could be taken beyond about 3.3 mm above the top of the burner because soot would clog the probe. Species mole fractions, X_i , were measured with a mass spectrometer and signal averaged on a computer. The complete species profiles were measured a number of

times. The resulting statistical uncertainties at the 90% confidence level (estimated from a Student's *t* distribution) were about $\pm 10\%$ for benzene. For styrene and phenylacetylene the uncertainty was about $\pm 25\%$ near their peaks and $\pm 50\%$ in the pre-flame zone where their concentrations were very low. There was also a potential systematic error of as much as 50% for styrene and phenylacetylene because of uncertainty in the mass spectrometer calibration. The pressure drop across the microprobe orifice was maintained at between 50:1 and 100:1 in order that the stable species chemistry would be adequately quenched. Tests and analysis on several species indicated that the quench was successful¹¹. We estimated that the profiles were shifted by approximately 2.5 probe orifice diameters (0.4 mm) from their true location¹¹. The figures in this paper have incorporated this shift. Temperatures were determined from measurements with both 3 mil and 5 mil diameter silica-coated, radiation-corrected Pt/Pt-Rh thermocouples. For measurements made in the sooting zone, thermocouple readings were difficult to take because the temperature dropped as soon as the thermocouple became coated with soot. Therefore, measurements were taken continuously with a computer as the flame was ignited. In this way the rise and fall in the thermocouple readings were recorded. We took the highest measured temperature as the true flame temperature, making sure that our results were unaffected by the rate at which the computer took the measurements. The two different thermocouples gave identical temperature profiles. The temperature peaked at 3.1 mm above the top of the burner at about 1640 K.

Concentration profiles were modeled using the Sandia burner code¹⁴ together with a mechanism that we developed for the flame. A number of reactions involving butane, butyl radical, 2-butene, propane, acetaldehyde, and acetaldehyde radical were considered, but they did not contribute to the profiles that we measured under our conditions. Therefore those species were eliminated. A partial mechanism is given in Table 1. (The complete mechanism is available from the authors.) For ease of comparison with previous work of Frenklach *et al.*^{10,15}, we have used the shorthand nomenclature that they suggested for aromatic species. In this system $A_n(R_m)$ refers to a species with *n* fused aromatic rings (fused to an *m*-membered non-aromatic ring). Radicals are indicated by a "*" or a "-". Table 2 shows structures for some of the species which appear in the mechanism. A complete table is given in Frenklach *et al.*¹⁵.

Most of the thermodynamics for small species comes from the Chemkin data base¹⁶, supplemented where necessary by other standard sources¹⁷. We assumed^{11,18a} a 70.5 kcal heat of formation for the vinyl radical (C_2H_3) and a 109 kcal heat of formation for C_4H_2 ^{18b}. For all the aromatic species we used the thermodynamics of Stein and Fahr¹⁹. (This set of data was called S6^{10,19b}.) In addition we used Stein and Fahr's thermodynamics for three aliphatic radicals which are closely related in our model to aromatic species, namely $n-C_4H_3$ ($\Delta H_f^{300} = 124$ kcal/mole), C_8H_5 ($\Delta H_f^{300} = 190$ kcal/mole), and C_6H_5 ($\Delta H_f^{300} = 138$ kcal/mole).

Information on the high temperature kinetics of most aromatic species, especially those larger than benzene, tends to be either too sparse or too tentative for us simply to use literature values for rate constants. In order to make progress we followed the approach of Frenklach, Clary, Gardiner, and Stein²⁰ (FCGS). These workers considered a very large number of elementary reactions for aromatic formation and growth. The reactions were grouped into classes, and all reactions of a given class were assigned the same rate constant.

For example, based on the measurement by Madronich and Felder²¹ for the rate of reaction between *OH* and benzene, all reactions involving *OH* abstraction of an aromatic hydrogen were assigned the rate constant $k_{T02} = 2.1 \times 10^{14} e^{-4600/RT}$. For other reaction classes rate constants were not available, and upper limit (nearly gas kinetic) values were assigned to their rate constants. In this way, they were able to identify the major reaction pathways as well as pathways which were not important.

However, use of upper limit values for rate constants entails certain disadvantages. First, because they are in general too large, this approach cannot be expected to yield results that are in quantitative agreement with experiment. Second, the usefulness of sensitivity coefficients cannot be expected to be great if the estimated rate constants are incorrect by very large factors. (However, FCGS²⁰ identified some pathways to aromatic formation whose relative importance is very small for almost any reasonable choice of rate constants.) Finally, if the rate constants are chosen to be sufficiently high the sensitivity coefficients may be smaller than they otherwise would be (As $k \rightarrow \infty$ its associated sensitivity coefficients will in general approach 0.), and the analysis may conclude that thermodynamics is relatively more important compared to kinetics than it actually is.

In our work we addressed these issues by using experimentally derived rate constants which have recently become available and by testing the effects of some very large changes in the rate constants (see Discussion section). The rate constants for aromatic species were derived as follows:

1. Mallard *et al.*²² measured the rate for reaction of the phenyl radical with acetylene (*U*15) and ethylene (*U*18). We used the same rate constants for *U*16, *U*17, *U*19, *U*20, and *G*10, which are similar.
2. Kiefer *et al.*²³ obtained the rate constant for abstraction of a benzene hydrogen by *H* (*T*03) from a model of his shock tube experiments. This rate constant extrapolates at 800 K to a value fairly close to that suggested by Nicovich and Ravishankara²⁴. We used the same value for *U*02, *G*02, and *G*11. We assumed that abstraction of an aromatic hydrogen by *C*₂*H* and *C*₂*H*₃ is five times slower (*G*04, *G*05, *G*08, *G*09, *U*04, *U*05, *U*09, and *U*10).
3. Colket²⁵ used his shock tube results to obtain the rate constant for the displacement of a benzene hydrogen by *C*₂*H* (*U*11). We used the same value for displacement by vinyl (*U*12). The value for *k*_{*T*06}, the rate constant for ring formation, is taken from FW¹⁰, which at our temperatures is nearly identical to the value estimated by Colket²⁵. *k*_{*U*21} and *k*_{*G*12} were given the same value.
4. Hsu *et al.*²⁶ measured the rate constant for decomposition of benzene to phenyl and *H* (*T*01). We used this value for *U*01, *U*06, *G*01, and *G*06.
5. Cole *et al.*^{5b} estimated the rate of formation of benzene from *C*₄*H*₅ and *C*₂*H*₂ in their low pressure butadiene flame. We used their value for *k*_{*T*07}.
6. The rate constant for *U*13 was given an upper limit value taken from Frenklach and Warnatz¹⁰; the same rate constant was used for *U*14.
7. *k*_{*T*08} and *k*_{*U*22} are evaluated below.

Reaction Path and Sensitivity Analysis

Principal reaction paths for species up to the *C*₄'s have been presented previously¹¹.

Graphs of the concentration profiles of many of those species were also presented¹¹. Here we discuss profiles and reaction paths for the single-ring aromatic species that we measured.

Benzene (A_1)

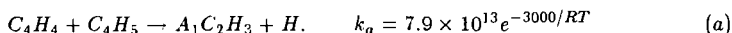
The calculated rate of benzene formation peaks between 1.6 and 2.2 mm (from 1450 - 1600 K), compared to peak formation rates of the C_3 and C_4 species between 1 and 1.6 mm. A single reaction path dominates at 1.8 mm, $T08$ followed by $T06$ and $-T01$ or $-T03$. The importance of $T08$ was emphasized originally by Bockhorn *et al.*⁶ and FCGS²⁰. In the pre-reaction zone $T07$ dominates, reflecting the higher concentration of C_4H_5 compared to $n-C_4H_3$ in the lower temperature environment found there (Figure 1). FW also found that ring formation was dominated by $T07$ in the pre-flame zone. We did not include any oxidation reactions which destroyed the aromatic ring since we have no evidence that such reactions are important in our flame and since the detailed kinetics of the species involved²⁷ would be entirely speculative.

A sensitivity analysis shows that the calculated benzene concentration in the region of its peak formation rate depends most strongly (sensitivity coefficient $\equiv \left| \frac{\partial \ln X_i}{\partial \ln k_j} \right| > 0.5$) on only three rate constants, k_{F01} , k_{A02} , and k_{T08} ; other rate constants to which the benzene concentration is sensitive include k_{H02} , k_{H03} , k_{A08} , k_{V04} , k_{V11} , and k_{F11} . k_{T01} and k_{T06} , with sensitivity coefficients between 0.05 and 0.06 are the only rate constants involving an aromatic ring with a sensitivity coefficient greater than 0.05. In the pre-flame region the above rate constants again have the highest sensitivities. Thus, among all the rate constants involving aromatic formation, many of whose values had to be guessed or extrapolated, only k_{T08} is critical. (This same conclusion was reached by FCGS²⁰ in their very extensive search for reaction paths leading to the formation of aromatic rings.) The calculated concentration is also sensitive to the thermodynamic values assumed for $n-C_4H_3$, a 5 kcal/mole increase in its heat of formation leading to a 3-fold reduction in the benzene concentration. A similar change in the assumed heat of formation of the aliphatic radical C_6H_5 has only a 10% effect. Assuming, then, that our pathway to form benzene is correct, that oxidation reactions which destroy the ring can be ignored, and that the thermodynamics is correct, we can estimate k_{T08} by comparing predicted and measured benzene concentrations. We chose $k_{T08} = k_{U22} = 1.5 \times 10^{12}$ cm³/molecule-sec, which is nearly identical to the value found¹⁰ to reproduce best the data of Bockhorn *et al.*⁶ (However, considering the differences between our mechanism and the one used in Ref. 10 as well as the differences in the pressure of the flames modeled, the significance of this agreement is not immediately clear.) With this choice, the rate of $T06$ at 1.8 mm is 50% faster than $-T06$, 2.5 times faster than $T08$, and about 10 times faster than $-T08$. Later in the flame, beyond 2.6 mm (1630-1640 K), the experiment shows that net benzene formation nearly comes to a halt. According to the model, in this region benzene is still being formed by $-T01$, but now it is being destroyed by $T03$ at about the same rate. Furthermore, $T06$ and $T08$ briefly run in the reverse (decomposition) directions, with the rate of $-T06$ being 0.6% faster than $T06$ and $-T08$ being 3.6% faster than $T08$. With such a fine balance, it is not surprising that the net directions in which $T06$, and $T08$ run are very sensitive to temperature. For example, our calculations show that if the peak temperature is assumed to be 1600 K, 40 K less than the measured value, these reactions always run in the direction of forming benzene.

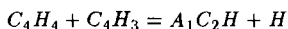
A comparison between the experiment and the model is shown in Figure 2. Adjustment of k_{T08} insures agreement at 3 mm, but we note that the model also reproduces fairly well the shape of the rise through the flame zone as well as the sharp leveling out in the profile beyond 2.5 mm.

Phenylacetylene (A_1C_2H) and Styrene ($A_1C_2H_3$)

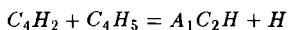
The predicted phenylacetylene profile (solid curve in Figure 3) differs by a factor of up to 6 from the experimentally measured profile. This discrepancy is more than a factor of two worse than for the C_3 and C_4 species from which phenylacetylene is ultimately formed, and it is much greater than the uncertainty in the measurements. Because all of the aromatic species showed similar first-order sensitivity coefficients to most of the same rate constants, no adjustment of a single rate constant to improve the agreement with phenylacetylene seemed possible without seriously degrading the agreement between the model and experiment for the other aromatic species. It is likely that the discrepancy is due to a combination of errors in more than one rate constant, requiring second- or higher-order sensitivity coefficients to identify them, or to errors in the precursor thermodynamics. However, we considered two alternate explanations for the discrepancy. First, we may not have identified the major pathway forming phenylacetylene. For example, Colket²⁵ has suggested an overall irreversible pathway to phenylacetylene.



Addition of these reactions increased the calculated phenylacetylene concentration by less than 10%, while reducing the styrene concentration by nearly an order of magnitude. Such a reduction would seriously degrade the agreement between measured and calculated styrene profiles (see below). (On the other hand, adding a detailed route from styrene to phenylacetylene analogous to the route from ethylene to acetylene—essentially a detailed version of Equation (b)—had hardly any effect on any of the aromatic profiles.) Inclusion of other possible routes to phenylacetylene,



or



with $k = 1.0 \times 10^{13}$ had little or no effect. Increasing k_{U22} by a factor of 5 had no effect on the phenylacetylene profile. We found no new reaction pathway which gave a substantial increase in the phenylacetylene concentration. A second possible explanation for the discrepancy between the model and the experiment could be uncertainty in the thermodynamics of phenylacetylene. To test for this possibility we lowered its assumed heat of formation at 300 K from 75 to 71 kcal/mole. The result, shown by the dashed line in Figure 3, is improved overall agreement, although the calculated and experimental profile shapes are still somewhat different. (The same effect could be obtained by changing the assumed entropy or the assumed heat capacity at high temperature.) Among other species, only the benzene and styrene concentrations were affected by this change, being reduced by about 10%.

The peak formation rate for phenylacetylene occurs in the same region as for benzene. Most of the phenylacetylene comes from the direct reaction between phenyl and acetylene (U_{15}); a smaller but still substantial amount comes from U_{22} followed by U_{21} and $-U_{09}$. The sensitivity coefficients for phenylacetylene are similar to those for benzene, although sensitivities to k_{F01} , k_{F08} , k_{F11} , k_{A02} , and k_{A08} are somewhat higher, reflecting among other factors a particular sensitivity to the acetylene concentration (which is modeled very well). There is also some sensitivity—about 0.1—to $k_{U_{15}}$. (But increasing $k_{U_{15}}$ to 1.0×10^{13} increases the phenylacetylene concentration by only about 10%.)

The calculated net styrene formation rate peaks between 1.4–1.7 mm (1300–1500 K), somewhat earlier than the other aromatics. This is because the principal reaction forming styrene, U_{18} , involves C_2H_4 , whose concentration is falling rapidly with height. $-U_{12}$ is the major destruction reaction there. By 2.25 mm the rate of $-U_{12}$ exceeds U_{18} by a factor of 3, causing the styrene mole fraction to fall. Sensitivity coefficients for styrene are very similar to those for phenylacetylene, except for a much lower sensitivity to $k_{U_{15}}$ and some sensitivity to $k_{U_{12}}$ and $k_{U_{18}}$.

A comparison between calculated and measured styrene mole fractions is shown in Figure 4. The agreement in shape and magnitude is good, although the calculated profile peaks earlier than the experimental one. It is interesting that the experiment showed benzene and phenylacetylene climbing rapidly through the reaction zone and then leveling off, while the styrene concentration peaks and falls. The model reproduces the proper qualitative behavior for all three species. The concentration of styrene falls in part because the mole fractions of ethylene and vinyl drop steeply through the post-flame region (*e.g.*, see Figure 1), increasing the net rate of $-U_{12}$ and decreasing the net rate of U_{18} . The most important reactions forming phenylacetylene (U_{15}) and benzene (T_{08}) run mainly in the forward direction throughout the flame, in part because the acetylene mole fraction does not change substantially in the post-flame region.

Naphthalene (A_2) and Acenaphthalene (A_2R_5)

Although we have no measurements for species larger than styrene, we continued the mechanism up to acenaphthalene in order that profiles of the species that we measured not become artificially high due to a lack of exit channels²⁸.

The path to larger aromatics funnels through phenylacetylene. Attack by H (U_{02}) (or OH (U_{03})) gives phenylacetylene radical, which almost irreversibly adds acetylene (G_{13}) and closes to form the naphthalene radical A_7^*X (G_{12}). This species can give naphthalene ($-G_{06}$ or $-G_{11}$) or react with acetylene (G_{10}) to give acenaphthalene.

Our analysis shows that the sensitivity spectra of naphthalene and acenaphthalene are very similar to that of phenylacetylene. In addition both are very sensitive to U_{02} and somewhat sensitive to G_{13} , while acenaphthalene is also quite sensitive to G_{10} .

Discussion

Comparison with Other Systems

Frenklach and Warnatz¹⁰ have very recently made the first detailed flame calculations to model the profiles of aromatic species in a flame. The flame modeled was a sooting ($\phi = 2.75$) 90 torr premixed acetylene flame studied by Bockhorn *et al.*⁶. Although they

obtained a certain qualitative agreement with Bockhorn's data, the calculated profiles of the aromatics declined precipitously in the post-flame gases, while the measured profiles dropped rather more slowly. The principal reason for this discrepancy¹⁰ comes from an apparent overestimate of the fragmentation rate of aromatic radicals *via* the reverse of reactions such as T06. It is possible that this overestimate is due to errors in the thermodynamic parameters, since those parameters determine the reverse reaction rates.

With the chosen value for k_{T08} , the measurements and calculations for benzene and styrene in our flame are in good agreement, both in the profile shapes and in their absolute values. The fact that the experimentally measured benzene and phenylacetylene concentrations do not decline in the post-flame region of our flame as they do in Bockhorn's flame can readily be explained by the fact that Bockhorn's flame is about 400 K hotter than ours. Graham *et al.*²⁹ interpreted the fall in the soot yield in their shock tube experiments for temperatures above 1800 K by postulating that at high temperatures the aromatic ring fragments more rapidly than it grows. Other data showing this "bell" have been explained in a similar way³⁰, and the aromatics in premixed flames may be subject to the same processes.

FCGS²⁰ have suggested that the driving force behind formation of larger aromatic species and soot is the superequilibrium of H atoms. They proposed R/K_{eq} as a measure of this superequilibrium, where $R = [H]^2/[H_2]$ and where $K_{eq} = [H_{eq}]^2/[H_2]$. They attributed the decline in the formation and growth rate of aromatics at long time to the decay of R/K_{eq} . We have plotted this ratio in Figure 2. The precipitous decline in R/K_{eq} to values below about 100 coincides very roughly with the slowdown in the formation of the benzene profile. However, our kinetic analysis and that of FW¹⁰ suggest that it is the increase in temperature through the reaction zone—leading to higher ring fragmentation rates—which is actually responsible for the cessation of net benzene and phenylacetylene formation. From this point of view, the fall in R/K_{eq} is simply a reflection of the fact that the temperature is rising in a region of constant or falling H -atom mole fraction. Furthermore, our model predicts that net benzene and phenylacetylene formation accelerates later in the flame where the temperature is lower, even though R/K_{eq} ultimately drops to about 2. (This secondary rise in net aromatic formation has previously been modeled¹⁰ and observed experimentally³¹.) The fact that net benzene and phenylacetylene formation is greater when $R/K_{eq} < 10$ than when $R/K_{eq} \sim 100$ suggests that the value of this ratio is not of fundamental significance in aromatic formation.

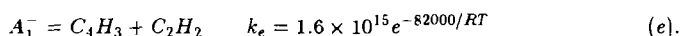
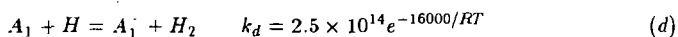
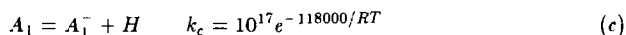
Robustness of the Model

The model that we have presented relies in many cases on analogies and estimates for rate constants of aromatic species because few of these rate constants are known. When they are measured the new values can replace those used here. Similarly, our knowledge of thermodynamic properties of large aromatic species can be expected to improve. The usefulness of this modeling effort, then, depends on the robustness of the calculations to potentially large changes in the values of the rate constants and to some changes in the thermodynamics. FW¹⁰ have shown the effects of changing certain thermodynamic assumptions, and we have reported above some effects on the calculated phenylacetylene profile. The effects are significant but not drastic for the species modeled here; additional efforts to measure or calculate thermodynamic properties, particularly for larger species,

would be very valuable in order to better understand hydrocarbon growth in flames.

The situation may be somewhat more promising with regard to uncertainty in the rate constants. The analyses done by FCGS²⁰, FW¹⁰, and ourselves show remarkably small values for most of the sensitivity coefficients. However, as we pointed out above, the model could still be quite sensitive to very large changes in the the rate constants. In order to evaluate this possibility, we ran our flame code using the aromatic mechanism and rate constants of FW, only adding analogous reactions for styrene, which did not appear in their mechanism, and using our value for k_{T08} . This involved many significant changes. For example, FW's value for k_{T03} is about two orders of magnitude greater than that of Kiefer *et al.*²³ The profiles for the single-ring compounds changed by less than 50% compared to those obtained using the mechanism in the Table 1, supporting our conclusion that k_{T08} is the only critical unknown rate constant. (However, the predicted concentrations of 2-ring compounds changed substantially, reflecting their sensitivity to $U02$.)

As a second test of the robustness of our mechanism we asked whether our model is consistent with benzene decomposition measurements made by Kiefer *et al.*²³ According to this proposed mechanism, benzene decomposition at 1 atmosphere follows the route:



Our mechanism already includes (d); we replaced $T01$ and $T06/T08$ with (c) and (e). The result is a reduction in the calculated aromatic concentration by 40-45%, with little effect on the qualitative shapes of the profiles. Since we have not used the same thermodynamic assumptions as Kiefer, use of his rate constants in our system is not really warranted. (The reactions are running in the reverse direction.) However, taken together with the fact that Kiefer's results were not highly sensitive to k_e , the modest effect of the change in rate constants suggests that the mechanism of Table 1 is in reasonable agreement with the shock tube results of Kiefer *et al.*

Conclusions

We believe that we have made progress in modeling the pyrolysis processes in our flame up to and including the formation of single-ring aromatic species, even though there is great uncertainty in many of the rate constants. Our sensitivity analysis shows that the basis for this success is that there is a single crucial unmeasured rate constant, k_{T08} , which largely controls the combined single-ring aromatic species concentrations. Our results are in accord with those of FCGS and FW, even though we used experimentally derived rate constants which were not available to them. The robustness of our model to future changes in most of the rate constants used in the aromatic part of our model appears to be high.

We hope in the future to continue our measurements and modeling work to species with more than one aromatic ring. If we are successful in modeling growth from one to two rings, we can have some hope for modeling much larger species if adequate thermodynamics are available.

The ability to model soot formation in a flame, however, requires overcoming several additional hurdles. First, the number of species becomes too large to handle with a code such as that used here. As an alternative we could model the growth to larger species by ignoring diffusion in the post-flame gases and using a much faster code which assumes a homogeneous environment. The burner code, then, would provide estimates for the concentrations of small radicals and hydrocarbons which could be crucial for the hydrocarbon growth. Second, in order to calculate soot particle inception, additional processes such as coagulation and surface growth would have to be included. Recent work³² suggests that these processes can be considered without significant additional demands on computer resources.

Acknowledgements

We are grateful to Professor Michael Frenklach of Pennsylvania State University for many helpful discussions and for providing us with an advance copy of his paper with Warnatz and with the thermodynamics of Stein and Fahr.

References

1. J. Warnatz, Twentieth Symposium (International) on Combustion, The Combustion Institute, p. 845 (1984).
2. Westbrook, C. K., Dryer, F. L., Schug, K. P., Nineteenth Symposium (International) on Combustion, The Combustion Institute, Pittsburgh, 1982, pg. 153.
3. Miller, J.A., Mitchell, R.E., Smooke, M.D., and Kee, R.J., Nineteenth Symposium (International) on Combustion, The Combustion Institute, p. 181 (1982).
4. Bonne, U., Homann, K.H., and Wagner, H.Gg., Tenth Symposium (International) on Combustion, The Combustion Institute, p. 503 (1965).
- 5a. Bittner, J.D. and Howard, J.B., Eighteenth Symposium (International) on Combustion, The Combustion Institute, p. 1105 (1982).
- b. Cole, J.A., Bittner, J.D., Longwell, J.P., and Howard, J.B. *Combustion and Flame* **56**, 51 (1984).
6. Bockhorn, H., Fetting, F., and Wenz, H.W., *Ber. Bunsenges. Phys. Chem.* **87** 1067 (1983).
7. Taylor, B.R., Thesis, Department of Chemical Engineering, MIT, 1984.
8. Warnatz, J., Bockhorn, H., Moser, A., and Wenz, H.W., Nineteenth Symposium (International) on Combustion, The Combustion Institute, Pittsburgh, p. 197 (1982).
9. Levy, J.M., Taylor, B.R., Longwell, J. P., and Sarofim, A. F., Nineteenth Symposium (International) on Combustion, The Combustion Institute, Pittsburgh, p. 167 (1982).
10. M. Frenklach and J. Warnatz, "Detailed Modeling of PAH Profiles in a Sooting Low-Pressure Acetylene Flame," *Combustion Science and Technology*, in press.
11. Harris, S.J., Weiner, A.M., Blint, R.J., and Goldsmith, J.E.M., Twenty-first Symposium (International) on Combustion, The Combustion Institute, in Press.
12. Cathonnet, M., Gaillard, F., Boettner, J. C., Cambray, P., Karmed, D., Bellet, J.C., "Twentieth Symposium (International) on Combustion", The Combustion Institute, Pittsburgh, 1984, pg. 819.
13. Harris, S.J., Weiner, A.M., Ashcraft, C.C., *Comb. and Flame* **64**, 65 (1986).
- 14a. Smooke, M.D., *J. Comp. Phys.*, **48**, 72 (1982).
- b. Kee, R.J., Grcar, J.F., Smooke, M.D., and Miller, J.A., "A Fortran Program for Modeling Steady Laminar One-Dimensional Premixed Flames." Sandia Report SAND85-8240, 1985.
15. Frenklach, M., Clary, D.W., Yuan, T., Gardiner, W.C., and Stein, S.E., *Combustion Science and Technology* **50**, 79 (1986).
16. Kee, R.J., Rupley, F.M., and Miller, J.A., "The Chemkin Thermodynamic Data Base," Sandia Report SAND87-8215, April, 1987.
- 17a. Stull, D.R., Westrum, E.F., and Sinke, G.C., "The Chemical Thermodynamics of Organic Compounds," Wiley, New York, 1969.
- b. Burcat, A. in "Combustion Chemistry," W.C. Gardiner, ed., Springer-Verlag, New York, 1984, p. 455.
- 18a. McMillen, D.F. and Golden, D.M., *Ann. Rev. Phys. Chem.* **33**, 493 (1982).

- b. Bittner, J.D., Thesis, MIT, 1981.
- 19a. Stein, S.E. and Fahr, A. J. Phys. Chem. **94**, 3714 (1985).
 - b. Frenklach, M., Clary, D.W., Gardiner, W.C., and Stein, S.E., 15'th Symposium on Shock Waves and Shock Tubes, Stanford University Press, 1986, p. 295.
20. Frenklach, M., Clary, D.W., Gardiner, W.C., and Stein, S.E., Twentieth Symposium (International) on Combustion, The Combustion Institute, p. 887 (1985).
21. Madronich, S. and Felder, W., J. Phys. Chem. **89**, 3556 (1985).
22. a. Mallard, W.G., Fahr, A., and Stein, S.E., Chem. Phys. Proc. Combustion, Paper 92, 1984.
 - b. Mallard, W.G., private communication.
23. Kiefer, J.H., Mizerka, L.J., Patel, M.R. and Wei, H.-C., J. Phys. Chem. **89**, 2013 (1985).
24. Nicovich, J.M. and Ravishankara, A.R., J. Phys. Chem. **88**, 2534 (1984).
25. Colket, M.B., "The Pyrolysis of Acetylene and Vinylacetylene in a Single-Pulse Shock Tube," Twenty-first Symposium (International) on Combustion, The Combustion Institute, in Press.
26. Hsu, D.S.Y., Lin, C.Y., and Lin, M.C., Twentieth Symposium (International) on Combustion, The Combustion Institute, p. 623 (1984).
27. Brezinsky, K., Prog. Energy Combust. Sci. **12**, 1 (1986).
28. Kiefer, J.H., Kapsalis, S.A., Al-Alami, M.S., Budach, K.A., Comb. and Flame **51**, 79 (1983).
29. Graham, S.C., Homer, J.B., and Rosenfeld, J.L., Proc. R. Soc. London **A344**, 259 (1975).
30. Frenklach, M., Ramachandra, M.K. and Matula, R.A., Twentieth Symposium (International) on Combustion, The Combustion Institute, p. 871 (1984).
31. Westmorland, P.R., "Experimental and Theoretical Analysis of Oxidation and Growth Chemistry in a Fuel-Rich Acetylene Flame," Ph. D. Thesis, Department of Mechanical Engineering, Massachusetts Institute of Technology, 1986.
32. Frenklach, M. and Harris, S.J., "Aerosol Dynamics Modeling Using the Method of Moments," J. Colloid and Interface Science, in Press.
33. Gardiner, W. C. and Troe, J., in "Combustion Chemistry," W.C. Gardiner, ed., Springer-Verlag, New York, 1984, p. 173.
34. Frank, P.I., Bhaskaran, K.A., and Just, T., Twenty-First Symposium (International) on Combustion, The Combustion Institute, in press.

Table 1



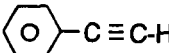
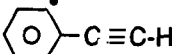
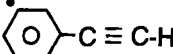
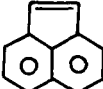
REACTIONS	A	n	E _a
A02) $C_2H_3 = C_2H_2 + H$	6.6E+19	-2.794	36130.0
A08) $C_2H_2 + OH = CH_2CO + H$	1.0E+14	0.0	11500.0
F01) $C_2H_3 + O_2 = HCO + CH_2O$	4.0E+12	0.0	-250.0
F11) $HCO + O_2 = CO + HO_2$	5.0E+11	0.5	835.0
H02) $H_2 + O = H + OH$	1.5E+07	2.0	7550.0
H03) $H + O_2 = O + OH$	1.2E+17	-.907	16620.0
V04) $C_4H_4 + H = C_4H_3 + H_2$	7.9E+13	0.0	14500.0
V11) $C_2H_2 + C_2H_2 = C_4H_3 + H$	2.0E+12	0.0	45900.0
T01) $A_1 = A_1^- + H$	5.0E+15	0.0	108600.0
T02) $A_1 + OH = A_1^- + H_2O$	2.1E+13	0.0	4600.0
T03) $A_1 + H = A_1^- + H_2$	2.5E+14	0.0	16000.0
T04) $A_1 + C_2H = A_1^- + C_2H_2$	5.0E+13	0.0	16000.0
T05) $A_1 + C_2H_3 = A_1^- + C_2H_4$	5.0E+13	0.0	16000.0
T06) $C_6H_5 = A_1^-$	1.0E+10	0.0	0.0
T07) $C_4H_5 + C_2H_2 = A_1 + H$	3.2E+11	0.0	3700.0
T08) $C_4H_3 + C_2H_2 = C_6H_5$	1.5E+12	0.0	0.0
U01) $A_1C_2H = A_1C_2H^* + H$	5.0E+15	0.0	108600.0
U02) $A_1C_2H + H = A_1C_2H^* + H_2$	2.5E+14	0.0	16000.0
U03) $A_1C_2H + OH = A_1C_2H^* + H_2O$	2.1E+13	0.0	4600.0
U04) $A_1C_2H + C_2H_3 = A_1C_2H^* + C_2H_4$	5.0E+13	0.0	16000.0
U05) $A_1C_2H + C_2H = A_1C_2H^* + C_2H_2$	5.0E+13	0.0	16000.0
U06) $A_1C_2H = A_1C_2H^- + H$	5.0E+15	0.0	108600.0
U07) $A_1C_2H + H = A_1C_2H^- + H_2$	2.5E+14	0.0	16000.0
U08) $A_1C_2H + OH = A_1C_2H^- + H_2O$	2.1E+13	0.0	4600.0
U09) $A_1C_2H + C_2H_3 = A_1C_2H^- + C_2H_4$	5.0E+13	0.0	16000.0
U10) $A_1C_2H + C_2H = A_1C_2H^- + C_2H_2$	5.0E+13	0.0	16000.0
U11) $A_1 + C_2H = A_1C_2H + H$	1.0E+12	0.0	0.0
U12) $A_1 + C_2H_3 = A_1C_2H_3 + H$	1.0E+12	0.0	0.0
U13) $A_1^- + C_2H = A_1C_2H$	1.0E+13	0.0	0.0
U14) $A_1^- + C_2H_3 = A_1C_2H_3$	1.0E+13	0.0	0.0
U15) $A_1^- + C_2H_2 = A_1C_2H + H$	3.2E+11	0.0	1350.0
U16) $A_1^- + C_4H_2 = A_1C_2H + C_2H$	3.2E+11	0.0	1350.0
U17) $A_1^- + C_4H_4 = A_1C_2H + C_2H_3$	3.2E+11	0.0	1350.0
U18) $A_1^- + C_2H_4 = A_1C_2H_3 + H$	3.2E+11	0.0	1900.0
U19) $A_1^- + C_4H_4 = A_1C_2H_3 + C_2H$	3.2E+11	0.0	1900.0
U20) $A_1^- + C_4H_6 = A_1C_2H_3 + C_2H_3$	3.2E+11	0.0	1900.0
U21) $C_8H_5 = A_1C_2H^-$	1.0E+10	0.0	0.0
U22) $C_4H_3 + C_4H_2 = C_8H_5$	1.5E+12	0.0	0.0
G01) $A_2R_5 = A_2R_5^- + H$	5.0E+15	0.0	108600.0
G02) $A_2R_5 + H = A_2R_5^- + H_2$	2.5E+14	0.0	16000.0
G03) $A_2R_5 + OH = A_2R_5^- + H_2O$	2.1E+13	0.0	4600.0

G04)	$A_2R_5 + C_2H = A_2R_5^- + C_2H_2$	5.0E+13	0.0	16000.0
G05)	$A_2R_5 + C_2H_3 = A_2R_5^- + C_2H_4$	5.0E+13	0.0	16000.
G06)	$A_2 = A_2^-X + H$	5.0E+15	0.0	108600.0
G07)	$A_2 + OH = A_2^-X + H_2O$	2.1E+13	0.0	4600.0
G08)	$A_2 + C_2H_3 = A_2^-X + C_2H_4$	5.0E+13	0.0	16000.0
G09)	$A_2 + C_2H = A_2^-X + C_2H_2$	5.0E+13	0.0	16000.0
G10)	$A_2^-X + C_2H_2 = A_2R_5 + H$	3.2E+11	0.0	1350.0
G11)	$A_2 + H = A_2^-X + H_2$	2.5E+14	0.0	16000.0
G12)	$A_1C_2HC_2H_2 = A_2^-X$	1.0E+10	0.0	0.0
G13)	$A_1C_2H^* + C_2H_2 = A_1C_2HC_2H_2$	1.0E+13	0.0	0.0

Units are cm³, moles, seconds, calories

Captions

1. Calculated mole fraction profiles for three radical species.
2. Left axis, benzene mole fraction. Symbols are experimental measurements, the curve is the model calculation. Right axis, calculated superequilibrium of H .
3. Phenylacetylene mole fraction. Symbols are experimental measurements, the solid curve is the model calculation, the dashed curve is the model calculation when the assumed heat of formation of phenylacetylene is lowered by 4 kcal/mole.
4. Styrene mole fraction. Symbols are experimental measurements, the solid curve is the model calculation.

<u>Structure</u>	<u>Name</u>
	A_1
	A_1^-
	A_1C_2H
	$A_1C_2H^*$
	$A_1C_2H^-$
	A_2R_5

